Electronic Supplementary Material (ESI) for Chemical Communications.
This journal is © The Royal Society of Chemistry 2021

Supporting Information

Tailoring the triplet level of isomorphic Eu/Tb mixed MOFs for sensitive temperature sensing

Tifeng Xia,*[a] Zhengfeng Shao,[a] Xiayan Yan,[a] Meng Liu,[a] Libing Yu,[a] Yating Wan,[c] Dingyue Chang,[a] Jun Zhang,*[a] and Dian Zhao*[b]

[a]*Institute of Materials, China Academy of Engineering Physics, Mianyang 621907, China. E-mail: xiatifeng@caep.cn, j-zhang@caep.cn*

[b]*Key Laboratory of the Ministry of Education for Advanced Catalysis Materials, Department of Chemistry, Zhejiang Normal University, Jinhua 321004, China. E-mail: dzhao@zjnu.edu.cn*

[c]*Shanghai Institute of Laser Plasma, China Academy of Engineering Physics, Shanghai 201800, China*

1. Experimental

1.1 Materials and Measurements

Materials: All reagents were obtained from commercial sources and used without further purification. 2-fluorobenzoic acid (2-FBA), 2-hydroxyterephthalic acid (H_2BDC-OH), 2-aminoterephthalic acid (H_2BDC-NH_2), 1,4-naphthalenedicarboxylic acid (1,4-H_2NDC), europium nitrate hexahydrate ($Eu(NO_3)_3 \cdot 6H_2O$), terbium nitrate hexahydrate ($Tb(NO_3)_3 \cdot 6H_2O$) and gadolinium nitrate hexahydrate ($Gd(NO_3)_3 \cdot 6H_2O$) were obtained from Energy Chemical (Shanghai, China).

Physical Measurements: Powder X-ray diffraction (PXRD) data were collected in the $2\theta = 5°–50°$ range on a PANalytical X'Pert Pro X-ray diffractometer using Cu-K_α ($\lambda = 1.542$ Å) beam at room temperature. The temperature-dependent emission spectra for the powders of Ln-MOFs were recorded on a Hitachi F4600 fluorescence spectrometer using Xe lamp as the light source. The phosphorescence spectra of Gd-based MOFs were measured by an Edinburgh Instrument F920 spectrometer using a μF900 lamp as the light source. UV-Vis absorption spectra of ligands in DMF were performed on UV-2600 spectrometer (Shimadzu Corp, Japan), the testing range was set from 200 to 700 nm. Thermogravimetric analyses (TGA) were conducted on a Netszch TGA 209 F3 thermogravimeter with a heating rate of 10 $K \cdot min^{-1}$ in N_2 atmosphere. The particle size and morphology was determined by a Hitachi S4800 Scanning Electron Microscope (SEM). Inductively coupled plasma spectroscopy (ICP) was performed on a Thermo IRIS Intrepid II XSP spectrometer.

1.2 Synthesis of of Ln-MOFs

Synthesis of LnBDC-OH: Taking EuBDC-OH as an example, 2-hydroxyterephthalic acid (H_2BDC-OH, 2,64 mg, 0.0145 mmol), $Eu(NO_3)_3 \cdot 6H_2O$ (6.47 mg, 0.0145 mmol), 2-fluorobenzoic acid (2-FBA, 16.23 mg, 0.116 mmol), *N,N'*-dimethylformamide (DMF, 730 μL), H_2O (60 μL), and HNO_3 (20 μL, 3.5 M in DMF) were sealed into a 5 mL Teflon cup. Then, the resulting solution was heated to 110 °C for 3 days and cooled to room temperature. The octahedral crystals of EuBDC-OH were collected and washed with DMF three times. $Eu_{0.01}Tb_{0.99}$BDC-OH, $Eu_{0.05}Tb_{0.95}$BDC-OH and GdBDC-OH were synthesized similarly to EuBDC-OH except for the use of a mixture of $Tb(NO_3)_3 \cdot 6H_2O$ and $Eu(NO_3)_3 \cdot 6H_2O$ or $Gd(NO_3)_3 \cdot 6H_2O$, respectively.

Synthesis of LnBDC-NH_2: EuBDC-NH_2 was synthesized by the solvothermal method. A mixture of $Eu(NO_3)_3 \cdot 6H_2O$ (323.4 mg, 0.725 mmol), 2-aminoterephthalic acid (H_2BDC-NH_2, 131.3 mg, 0.725 mmol), 2-fluorobenzoic acid (2-FBA, 812.6 mg, 5.8 mmol), DMF (36.5 mL), H_2O (3 mL), and HNO_3 (2 mL, 3.5 M in DMF)

was added to a 100 mL Teflon-lined stainless steel reactor, heated at 110 °C for 60 h, and then slowly cooled to room temperature. The colorless crystals of EuBDC-NH_2 were collected and washed with DMF. $Eu_{0.01}Tb_{0.99}$BDC-NH_2, $Eu_{0.005}Tb_{0.995}$BDC-NH_2 and GdBDC-NH_2 were synthesized similarly to EuBDC-NH_2 by using a mixture of $Tb(NO_3)_3 \cdot 6H_2O$ and $Eu(NO_3)_3 \cdot 6H_2O$ or $Gd(NO_3)_3 \cdot 6H_2O$, as the starting lanthanide salts, respectively.

Synthesis of LnNDC: EuNDC was solvothermally synthesized using the following method. 1,4-H_2NDC (9.41 mg, 0.0435 mmol), $Eu(NO_3)_3 \cdot 6H_2O$ (19.4 mg, 0.0435 mmol), and 2-FBA (48.7 mg, 0.348 mmol) were dissolved in a mixture of DMF (2.2 mL), H_2O (0.5 mL), and HNO_3 (0.3 mL, 3.5 M in DMF). The solution is sealed in a 20 mL Teflon cup and heated to 115 °C for 60 hours then cooled to room temperature. The colourless polyhedral crystals were collected and washed with DMF and dried at room temperature. $Eu_{0.01}Tb_{0.99}$NDC, $Eu_{0.0005}Tb_{0.9995}$NDC and GdNDC were synthesized similarly to EuNDC by using a mixture of $Tb(NO_3)_3 \cdot 6H_2O$ and $Eu(NO_3)_3 \cdot 6H_2O$ or $Gd(NO_3)_3 \cdot 6H_2O$, as the starting lanthanide salts, respectively.

2. Tables and Figures

Table S1 The molar ratio of the starting Eu/Tb salt and that in isomorphic Eu^{3+}/Tb^{3+} co-doped MOFs calculated by ICP analyses.

Samples	Tested Eu by ICP analysis (ppm)	Tested Tb by ICP analysis (ppm)	The Eu/Tb ratios calculated by ICP analysis
$Eu_{0.01}Tb_{0.99}$BDC-OH	0.68	34.43	0.0194:0.9806
$Eu_{0.01}Tb_{0.99}$BDC-NH_2	0.15	8.21	0.0179:0.9821
$Eu_{0.01}Tb_{0.99}$NDC	0.60	34.09	0.0173:0.9827

Table S2 The singlet and triplet energy level of three ligands.

Ligands	S_1 (cm^{-1})	T_1 (cm^{-1})
H_2BDC-OH	30959	24155
H_2BDC-NH_2	28409	21277
1,4-H_2NDC	32415	20161

Tb ($^5D_4$) 20430 cm^{-1} Eu ($^5D_0$) 17300 cm^{-1}

Table S3 Fitting parameters of isomorphic Eu^{3+}/Tb^{3+} mixed MOFs with empirical sigmoidal Boltzmann Origin8.0 built-in function.

MOFs	Thermometric parameter	A_1	A_2	x_o	dx	R^2
$Eu_{0.01}Tb_{0.99}$BDC-OH	Δ (I_{Tb}/I_{Eu})	10.5435	1.27121	128.27589	21.61000	0.99858
$Eu_{0.05}Tb_{0.95}$BDC-OH	Δ (I_{Tb}/I_{Eu})	2.33308	0.2564	129.86212	32.49366	0.99993
$Eu_{0.01}Tb_{0.99}$BDC-NH_2	Δ (I_{Tb}/I_{Eu})	0.06213	1.44115	192.25332	26.36044	0.99876
$Eu_{0.005}Tb_{0.995}$BDC-NH_2	Δ (I_{Tb}/I_{Eu})	0.02679	113.51387	411.06629	43.46826	0.99481
$Eu_{0.01}Tb_{0.99}$NDC	Δ (I_{Eu}/I_{NDC})	28.83290	2.35628	38.47376	7.58088	0.99886
$Eu_{0.0005}Tb_{0.9995}$NDC	Δ (I_{Eu}/I_{NDC})	305.69263	0.47043	-115.41722	233.87621	0.99899

Table S4. Comparing the performance of the Ln-MOF thermometers in terms of temperature range, maximum relative sensitivity (S_m) and corresponding temperature (T_m).

MOFs	Range (K)	S_m (% K^{-1})	T_m (K)	Ref.
$Tb_{0.99}Eu_{0.01}(bdc)_{1.5}$	290~320	0.31	318	1
$Tb_{0.995}Eu_{0.005}$@In(OH)(bpydc)	283~333	4.47	333	2
ZJU-88⊃perylene	293~353	1.28	293	3
Eu@UiO-(bpydc)	293~353	0.31	293	4
$Tb_{0.80}Eu_{0.20}$(bpda)	303~328	2.84	328	5
$Nd_{0.577}Yb_{0.423}$BDC-F_4	293~313	1.20	313	6
$Nd_{0.866}Yb_{0.134}$BTB	303~313	4.75	333	7
$Nd_{0.5}Yb_{0.5}$TPTC	293~328	12.46	293	8
$Tb_{0.99}Eu_{0.01}$(pia)	100~300	2.75	300	9
$Eu_{0.0005}Gd_{0.9995}$NDC	293~333	3.41	310	10
$Eu_{0.01}Tb_{0.99}$BDC-OH	313~513	2.24	425	This work
$Eu_{0.05}Tb_{0.95}$BDC-OH	313~513	1.55	440	This work
$Eu_{0.01}Tb_{0.99}$BDC-NH_2	313~473	2.49	426	This work
$Eu_{0.005}Tb_{0.995}$BDC-NH_2	313~473	2.22	473	This work
$Eu_{0.01}Tb_{0.99}$NDC	293~333	7.32	321	This work
$Eu_{0.0005}Tb_{0.9995}$NDC	293~333	3.16	283	This work

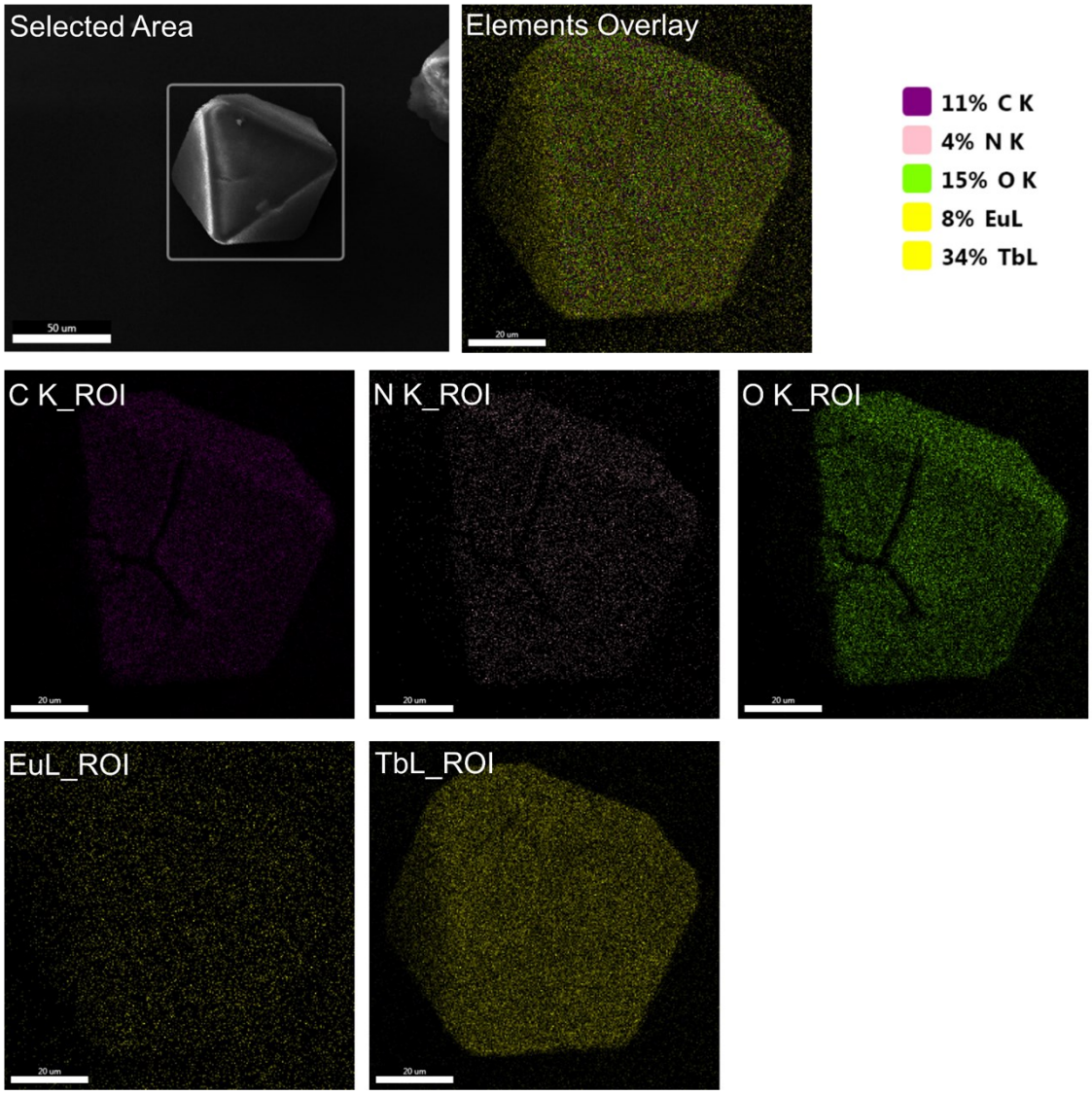

Fig. S1 EDS mapping of $Eu_{0.01}Tb_{0.99}BDC\text{-}NH_2$.

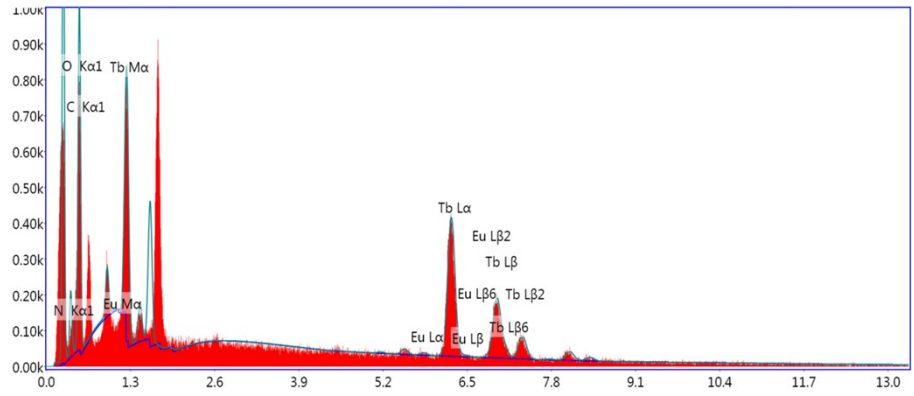

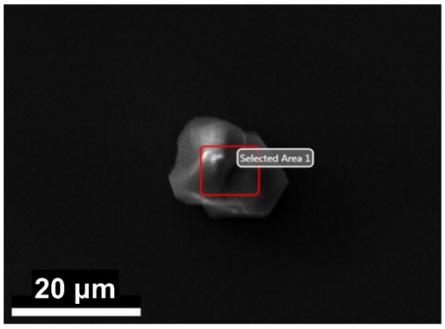

Elements	Weight ratio (%)	Atomic ratio (%)	Signal intensity
C K	31.40	49.80	614.51
N K	11.29	15.36	78.63
O K	26.12	31.10	485.09
EuL	0.59	0.07	10.95
TbL	30.60	3.67	541.00

Fig. S2 The elemental composition of $Eu_{0.01}Tb_{0.99}$BDC-OH determined by EDS.

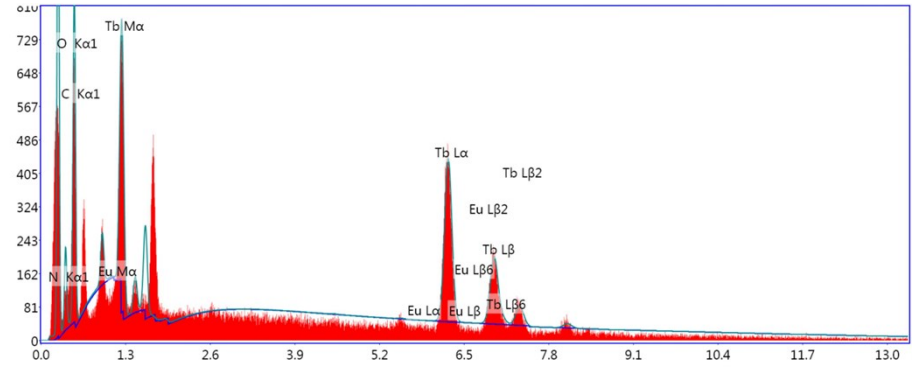

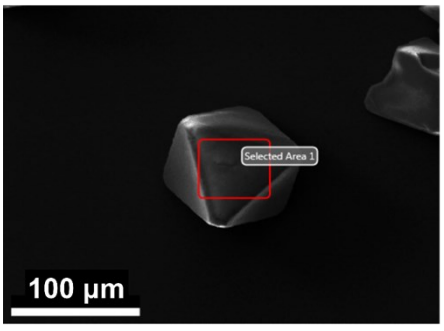

Elements	Weight ratio (%)	Atomic ratio (%)	Signal intensity
C K	29.24	49.37	518.97
N K	12.17	17.62	82.59
O K	22.40	28.38	388.60
EuL	0.44	0.06	7.81
TbL	35.74	4.56	597.60

Fig. S3 The elemental composition of $Eu_{0.01}Tb_{0.99}$BDC-NH_2 determined by EDS.

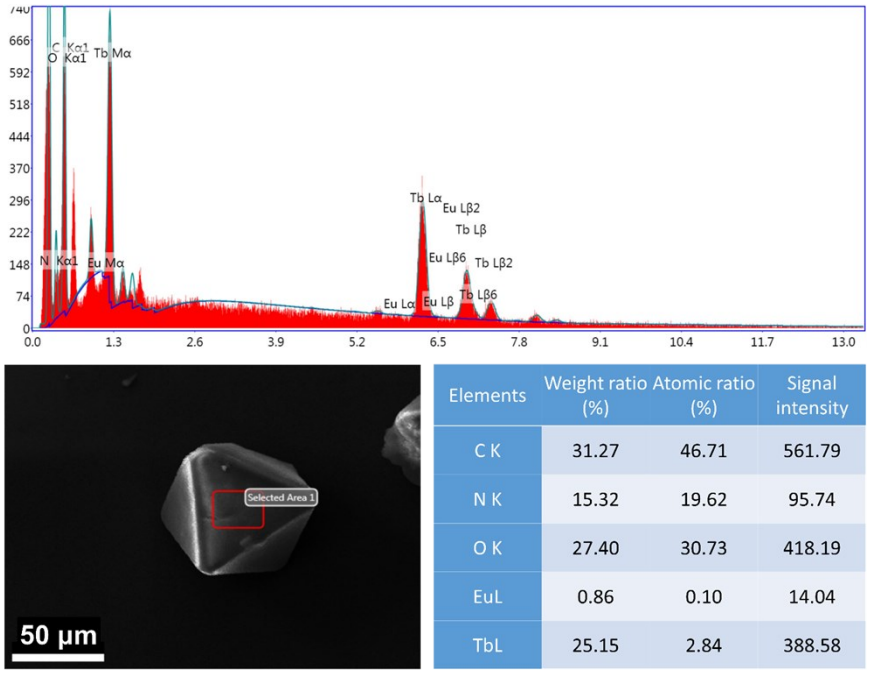

Elements	Weight ratio (%)	Atomic ratio (%)	Signal intensity
C K	31.27	46.71	561.79
N K	15.32	19.62	95.74
O K	27.40	30.73	418.19
EuL	0.86	0.10	14.04
TbL	25.15	2.84	388.58

Fig. S4 The elemental composition of $Eu_{0.01}Tb_{0.99}NDC$ determined by EDS.

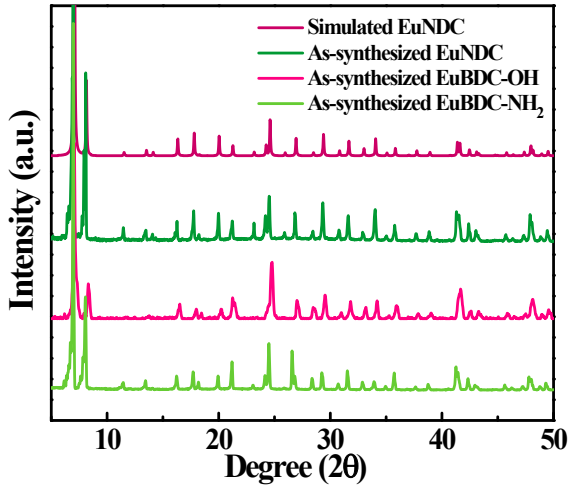

Fig. S5 PXRD patterns of simulated EuNDC and as-synthesized EuNDC, EuBDC-OH, and EuBDC-NH_2.

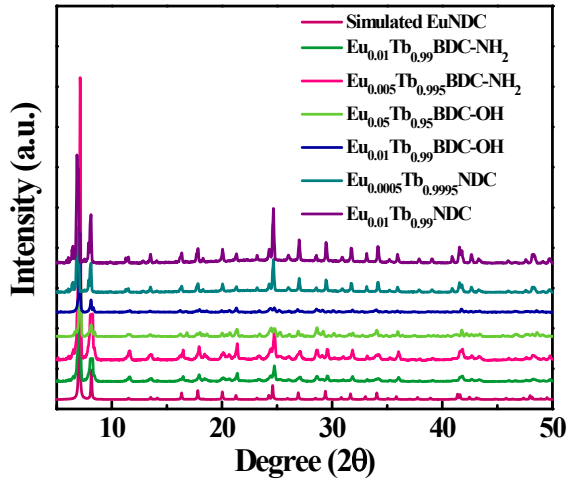

Fig. S6 PXRD patterns of as-synthesized $Eu_{0.01}Tb_{0.99}$BDC-OH, $Eu_{0.05}Tb_{0.95}$BDC-OH, $Eu_{0.01}Tb_{0.99}$BDC-NH_2, $Eu_{0.005}Tb_{0.995}$BDC-NH_2, $Eu_{0.01}Tb_{0.99}$NDC, and $Eu_{0.0005}Tb_{0.9995}$NDC.

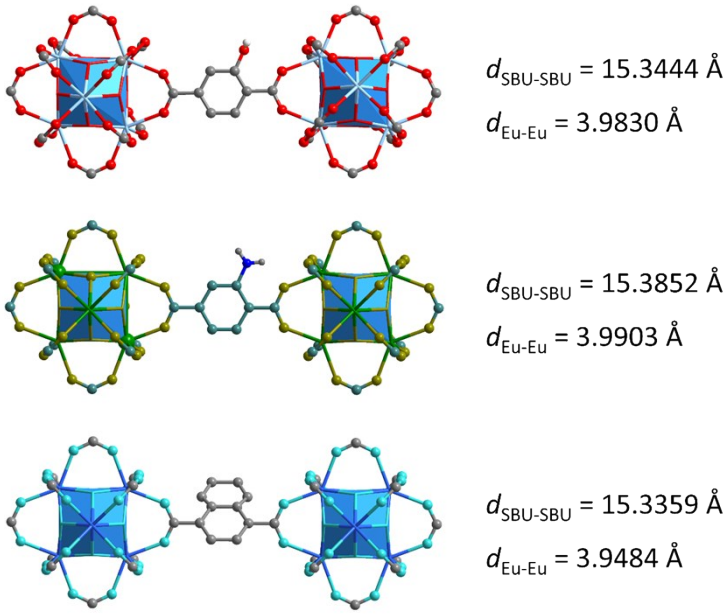

Fig. S7 The shortest distances between SBUs and between Ln atoms in EuBDC-OH, EuBDC-NH_2 and EuNDC, respectively.

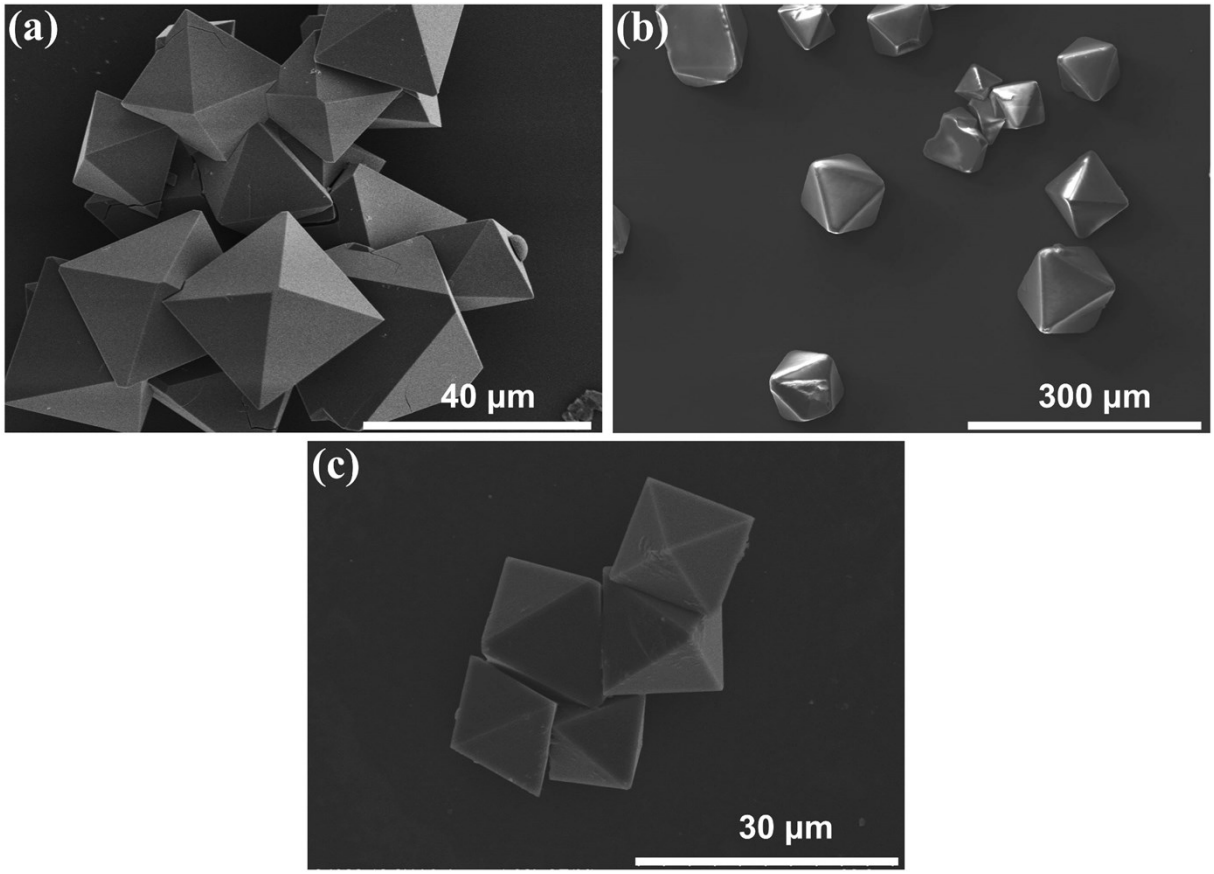

Fig. S8 SEM images of (a) EuBDC-OH, (b) EuBDC-NH_2 and (c) EuNDC.

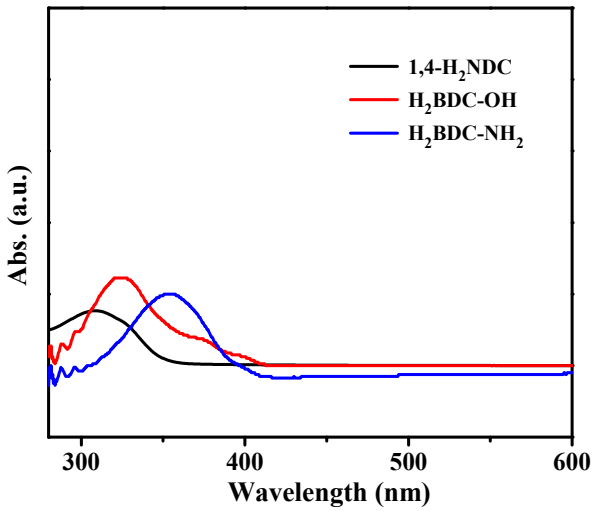

Fig. S9 UV-vis adsorption spectra of three organic ligands in DMF (1×10^{-4} mol L^{-1}) at room temperature.

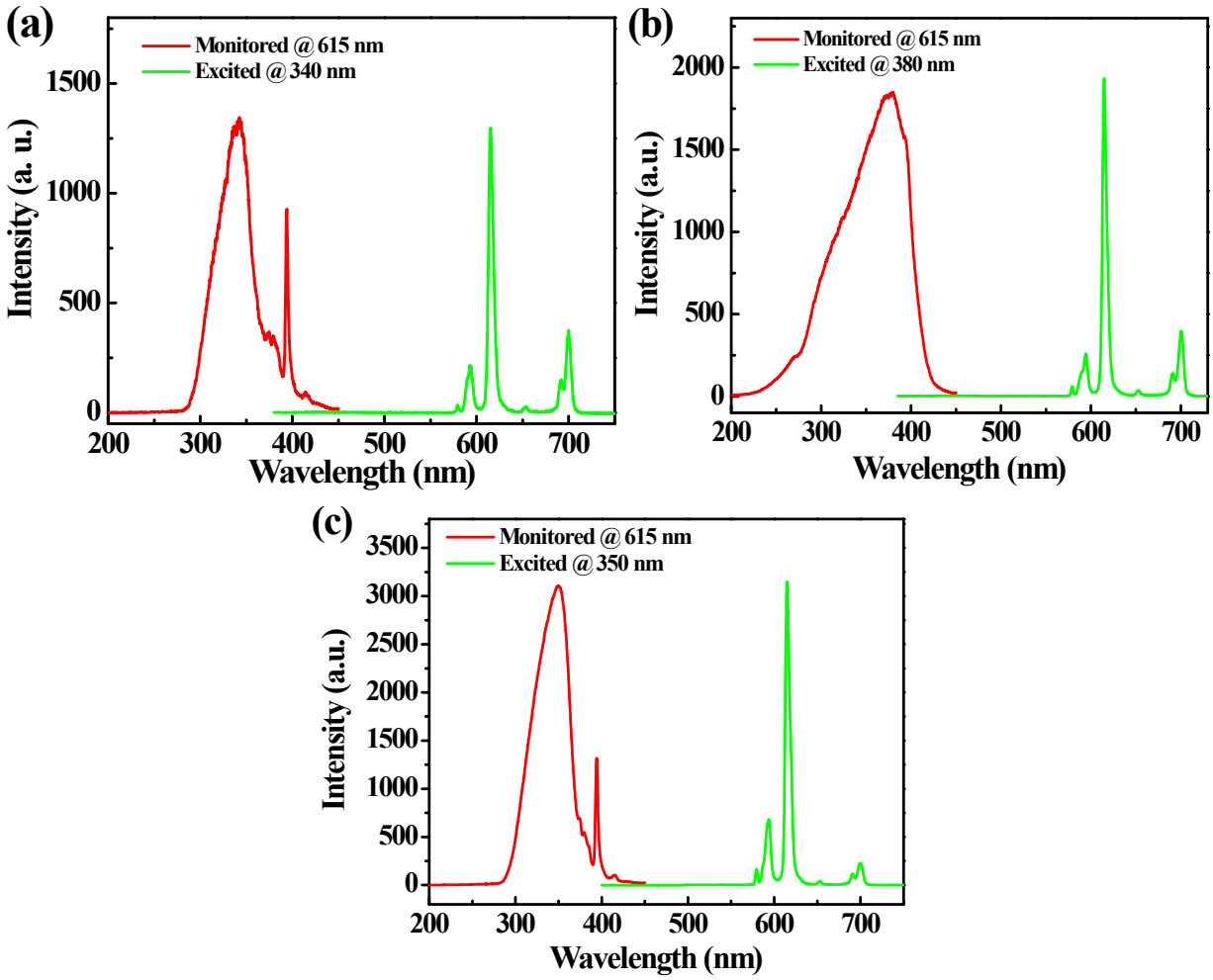

Fig. S10 The excitation and emission spectra of (a) EuBDC-OH, (b) EuBDC-NH_2 and (c) EuNDC in solid state.

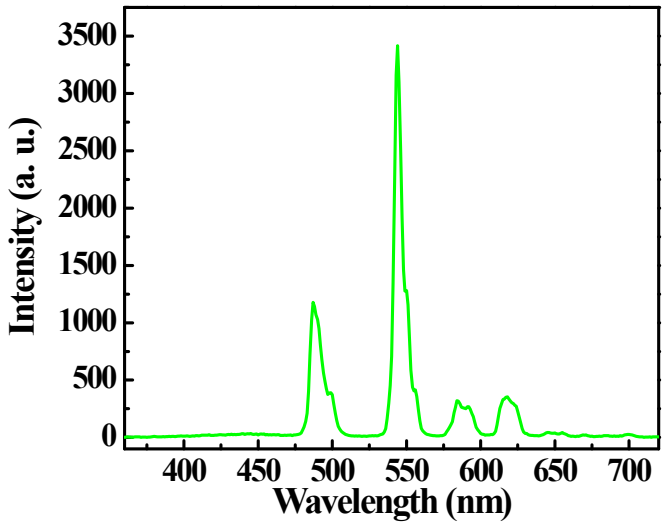

Fig. S11 The emission spectrum of $Eu_{0.01}Tb_{0.99}$BDC-OH upon excitation of 340 nm at room temperature.

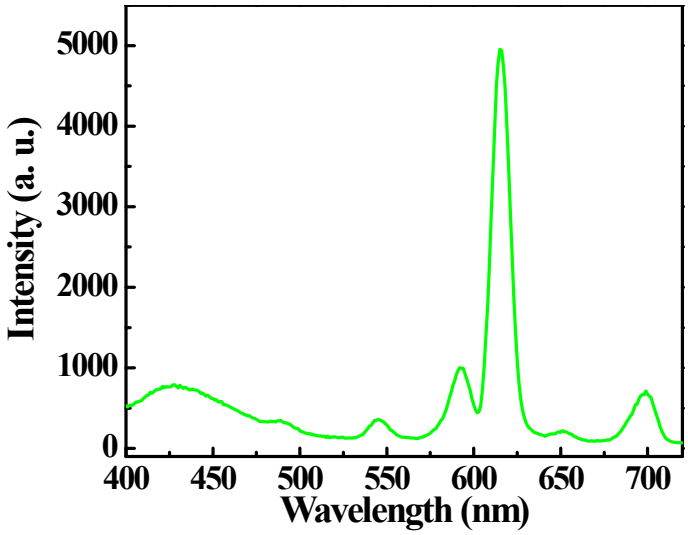

Fig. S12 The emission spectrum of $Eu_{0.01}Tb_{0.99}$BDC-NH_2 upon excitation of 375 nm at room temperature.

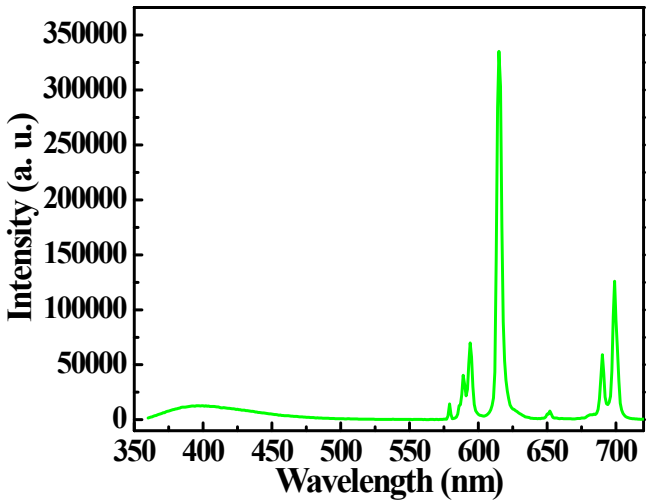

Fig. S13 The emission spectrum of $Eu_{0.01}Tb_{0.99}$NDC upon excitation of 350 nm at room temperature.

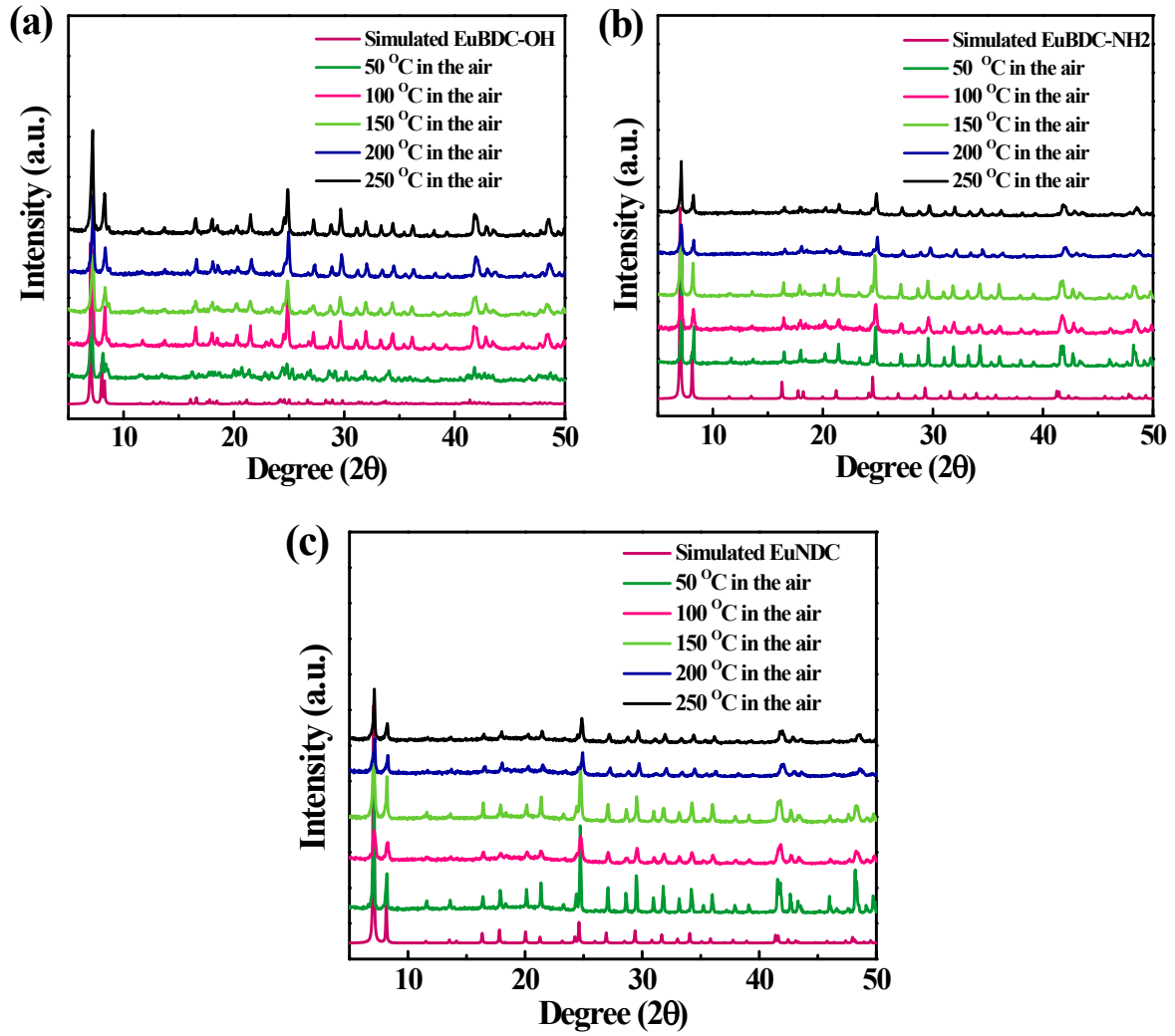

Fig. S14 PXRD patterns of (a) $Eu_{0.01}Tb_{0.99}$BDC-OH, (b) $Eu_{0.01}Tb_{0.99}$BDC-NH_2 and (c) $Eu_{0.01}Tb_{0.99}$NDC after different temperature treatment.

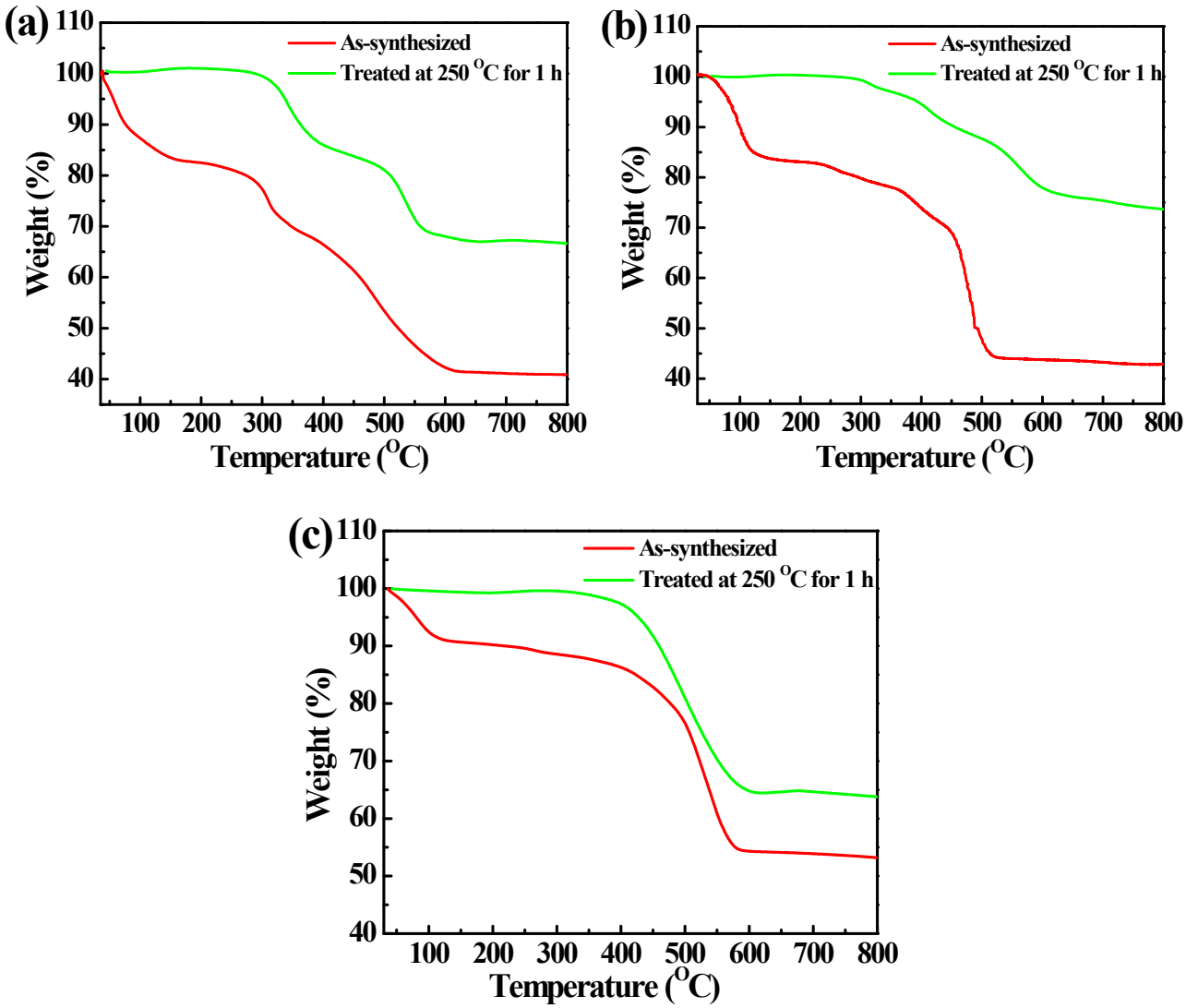

Fig. S15 TGA curves of (a) $Eu_{0.01}Tb_{0.99}$BDC-OH, (b) $Eu_{0.01}Tb_{0.99}$BDC-NH_2 and (c) $Eu_{0.01}Tb_{0.99}$NDC.

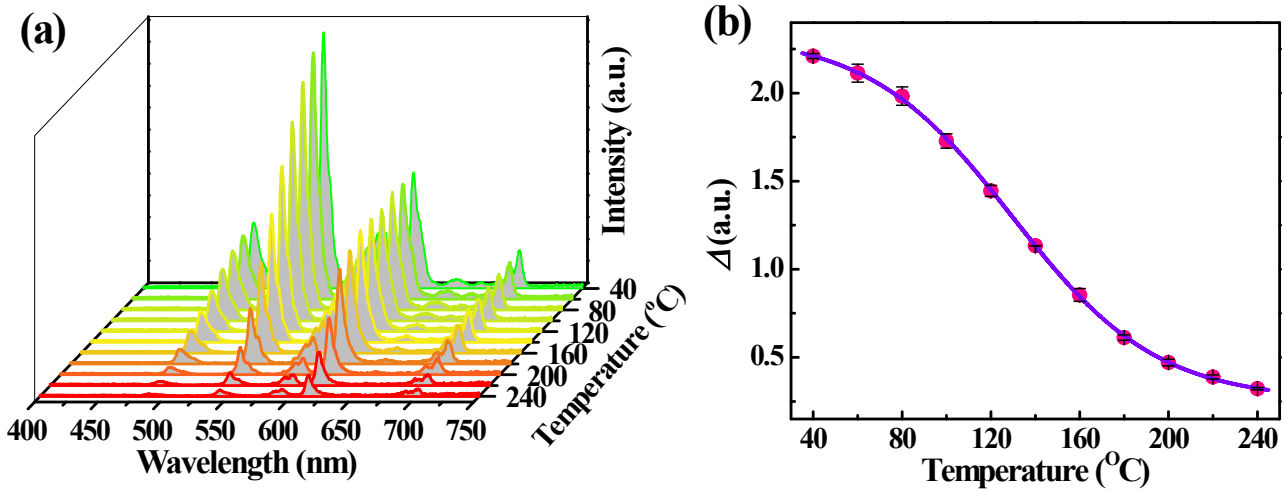

Fig. S16 Temperature-dependent emission spectra and thermometric parameter Δ ($\Delta = I_{Tb}/I_{Eu}$) of $Eu_{0.05}Tb_{0.95}$BDC-OH.

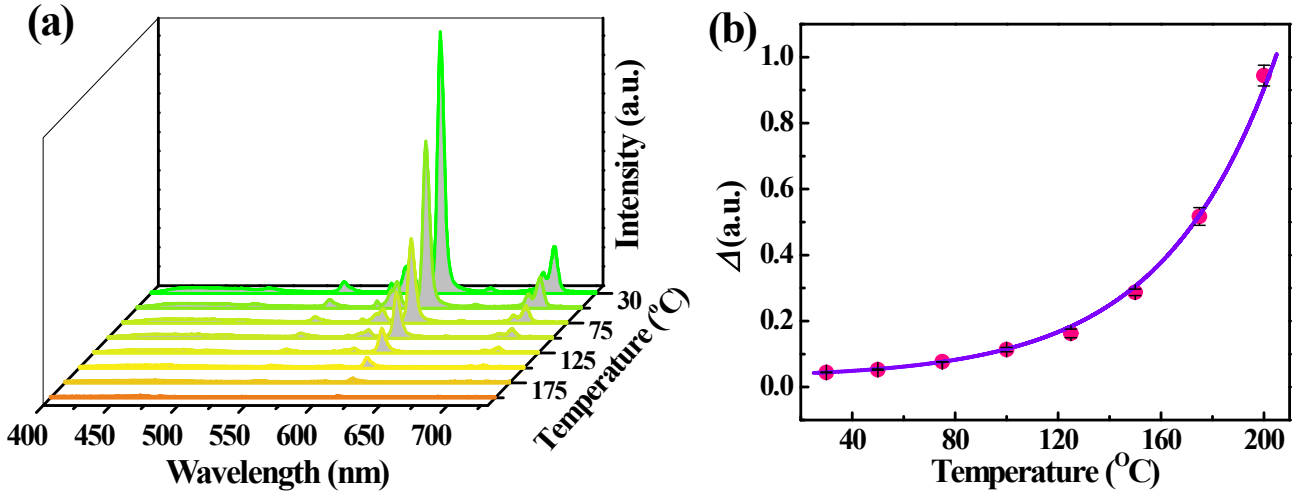

Fig. S17 Temperature-dependent emission spectra and thermometric parameter Δ ($\Delta = I_{Tb}/I_{Eu}$) of $Eu_{0.005}Tb_{0.995}BDC\text{-}NH_2$.

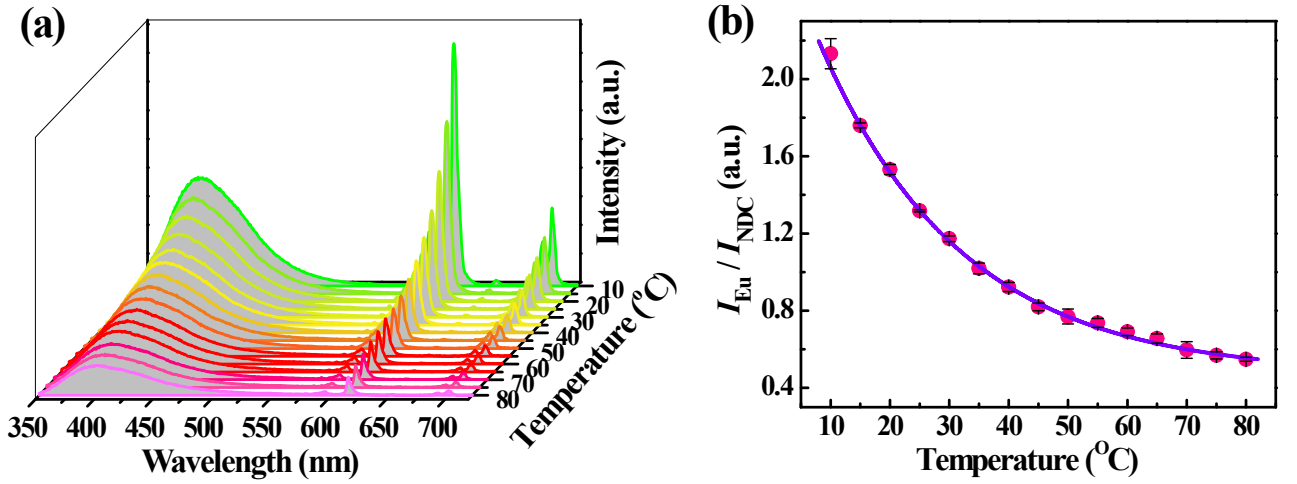

Fig. S18 Temperature-dependent emission spectra and thermometric parameter (I_{Eu}/I_{NDC}) of $Eu_{0.0005}Tb_{0.9995}NDC$.

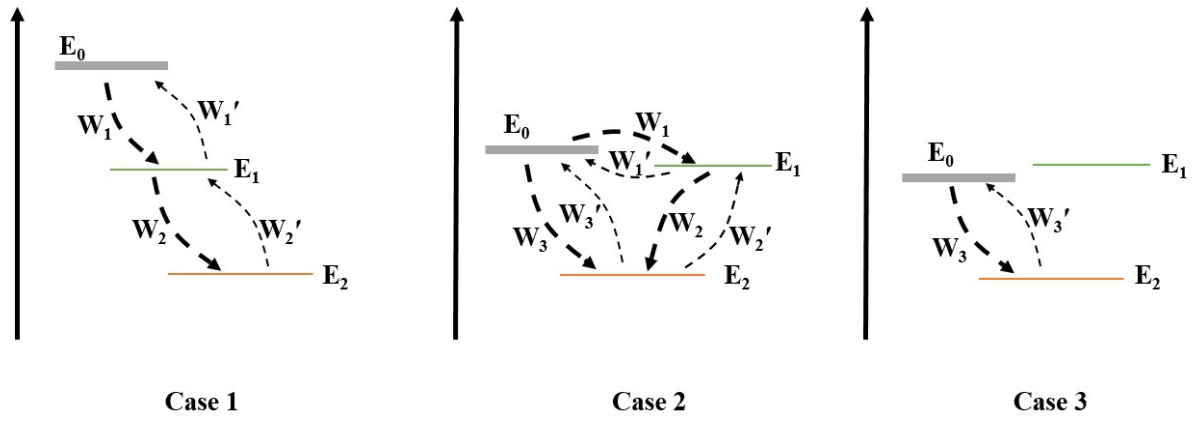

Fig. S19 The possible energy processes within $Eu_{0.01}Tb_{0.99}BDC\text{-}OH$ (Case 1), $Eu_{0.01}Tb_{0.99}BDC\text{-}NH_2$ (Case 2) and $Eu_{0.01}Tb_{0.99}NDC$ (Case 3).

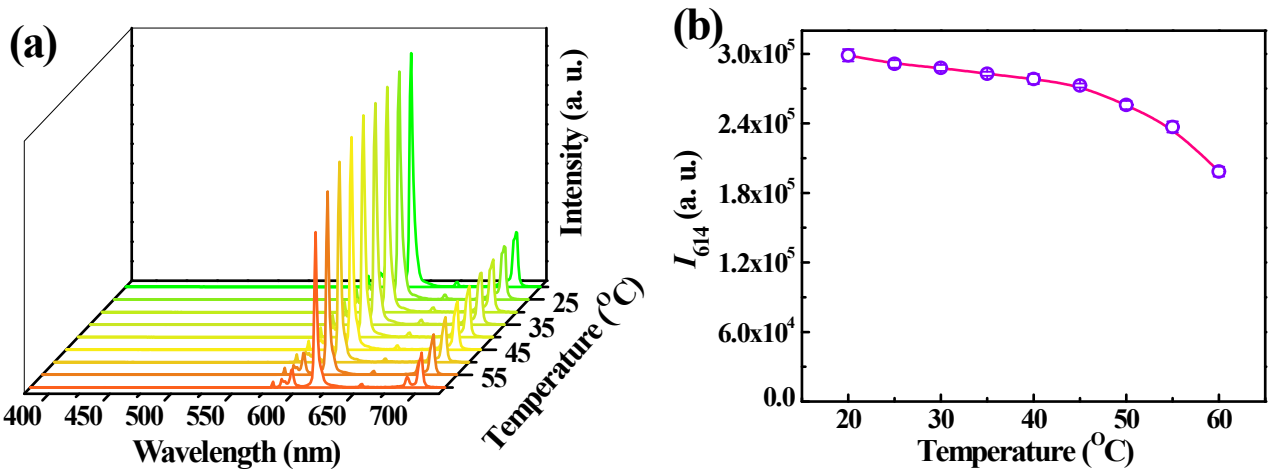

Fig. S20 (a) Temperature-dependent emission spectra of EuNDC in the physiological temperature range from 20 to 60 °C. (b) Temperature-dependent integrated intensity of Eu^{3+} emission at 614 nm.

The energy transfer rate from ligand to Tb is W_1, from Tb to Eu is W_2 and from ligand to Eu is W_3, and their corresponding back energy transfer rates are W_1', W_2' and W_3', and the energy distribution of ligands, Tb and Eu are E_0, E_1, and E_2, respectively. According to Boltzmann law, W_i' can be defined as

$$W_i' = W_i e^{-\frac{\Delta E}{k_B T}} \qquad \text{* MERGEFORMAT (1)}$$

where ΔE is the energy gap between donor and acceptor, k_B is the Boltzmann constant. The energy distribution and transfer processes model in three cases can be analyzed as follows.

Case 1:

$$E_2 = E_1(W_2 - W_2') \qquad \text{* MERGEFORMAT (2)}$$

$$E_1 = E_0(W_1 - W_1') - E_2 \qquad \text{* MERGEFORMAT (3)}$$

Case 2:

ΔE[T_1(H_2BDC-NH_2)-$^5D_4$(Tb)] is calculated as 847 cm^{-1}, W_1' almost equals to W_1.

$$E_2 = (E_0 - E_1)(W_3 - W_3') + E_1(W_2 - W_2') = (E_0 - E_1)(W_3 - W_3') + E_1(W_2 - W_2' + W_3' - W_3) \qquad \text{* MERGEFORMAT (4)}$$

Case 3:

$$E_2 = (W_3 - W_3')E_0 \qquad \text{* MERGEFORMAT (5)}$$

3. References

1. A. Cadiau, C. D. S. Brites, P. M. F. J. Costa, R. A. S. Ferreira, J. Rocha and L. D. Carlos, *ACS Nano*, 2013, **7**, 7213–7218.
2. Y. Zhou, B. Yan and F. Lei, *Chemical Communications*, 2014, **50**, 15235–15238.
3. Y. Cui, R. Song, J. Yu, M. Liu, Z. Wang, C. Wu, Y. Yang, Z. Wang, B. Chen and G. Qian, *Advanced Materials*, 2015, **27**, 1420–1425.
4. Y. Zhou and B. Yan, *Journal of Materials Chemistry C*, 2015, **3**, 9353–9358.

5. D. Zhao, X. Rao, J. Yu, Y. Cui, Y. Yang and G. Qian, *Inorganic Chemistry*, 2015, **54**, 11193–11199.
6. X. Lian, D. Zhao, Y. Cui, Y. Yang and G. Qian, *Chemical Communications*, 2015, **51**, 17676–17679.
7. D. Zhao, J. Zhang, D. Yue, X. Lian, Y. Cui, Y. Yang and G. Qian, *Chemical Communications*, 2016, **52**, 8259–8262.
8. D. Zhao, X. Han, S. Wang, J. Liu, Y. Lu and C. Li, *Chemistry- A European Journal*, 2019, **26**, 3145–3151.
9. X. Rao, T. Song, J. Gao, Y. Cui, Y. Yang, C. Wu, B. Chen, G. Qian, *Journal of the American Chemical Society*, 2013, **135**, 15559–15564.
10. T. Xia, J. Wang, K. Jiang, Y. Cui, Y. Yang and G. Qian, *Chinese Chemical Letters*, 2018, **29**, 861–864.